


## Article

# Synergic Combination of Hardware and Software Innovations for Energy Efficiency and Process Control Improvement: A Steel Industry Application

Silvia Maria Zanolì <sup>1,\*</sup> , Crescenzo Pepe <sup>1</sup>  and Lorenzo Orlietti <sup>2</sup>

<sup>1</sup> Dipartimento di Ingegneria dell'Informazione, Università Politecnica delle Marche, Via Brecce Bianche 12, 60131 Ancona, Italy; c.pepe@univpm.it

<sup>2</sup> Alperia Green Future, Via Dodiciville 8, 39100 Bolzano, Italy

\* Correspondence: s.zanoli@univpm.it

**Abstract:** The present paper proposes a steel industry case study focused on a reheating furnace and a rolling mill. Hardware and software innovations were successfully combined in order to obtain process control and energy efficiency improvement. The reheating furnace at study is pusher type and processes billets. The hardware innovation is related to the installation of an insulated tunnel at the end of the reheating furnace, in order to guarantee a higher heat retention of the billets before their path along the rolling mill stands. The software innovation refers to the design and the installation of an Advanced Process Control system which manipulates the gas flow rate and the stoichiometric ratio of the furnace zones in order to satisfy the control specifications on billets and furnace variables. The control system is based on Model Predictive Control strategy and on a virtual sensor which tracks and estimates the billet features inside/outside the furnace. The designed controller was commissioned on the real plant, providing significant performances in terms of service factor, process control, and energy efficiency.

**Keywords:** hardware innovation; software innovation; energy efficiency; Advanced Process Control; model predictive control; steel industry; rolling mill; reheating furnace; billets; insulated tunnel



**Citation:** Zanolì, S.M.; Pepe, C.; Orlietti, L. Synergic Combination of Hardware and Software Innovations for Energy Efficiency and Process Control Improvement: A Steel Industry Application. *Energies* **2023**, *16*, 4183. <https://doi.org/10.3390/en16104183>

Academic Editor: Boris Igor Palella

Received: 3 April 2023

Revised: 10 May 2023

Accepted: 17 May 2023

Published: 18 May 2023



**Copyright:** © 2023 by the authors. Licensee MDPI, Basel, Switzerland. This article is an open access article distributed under the terms and conditions of the Creative Commons Attribution (CC BY) license (<https://creativecommons.org/licenses/by/4.0/>).

## 1. Introduction

In the last decades, carbon dioxide (CO<sub>2</sub>) emission abatement attained an increasing rank within the goals of the energy-intensive industries. The reduction of the required energy usually infers a CO<sub>2</sub> emissions decrease; that is an inspiring and challenging target of the present energy transition in order to implement sustainability strategies. The goal to decrease CO<sub>2</sub> emissions has become a key target for the achievement of the objectives defined for 2030 and 2050 [1,2]. A fundamental role in this context is played by the “hard-to-abate” sectors, that is, those that rely on fossil fuels for the triggering of the processes involved [3,4]. A lot of energy (thermal and electrical) is required in many energy-intensive plants, e.g., steel and cement plants; in these plants, global revamping procedures could be adopted based on the substitution of the exploited resources. On the other hand, hardware and/or software upgrades can be performed which maintain the previously utilized resources but guarantee an improved, rational usage of them [5–7].

Among metallurgical industries, steel industry is of primary importance in the national and international context. Steel industry includes different production processes like, e.g., blast furnaces, as well as reheating furnaces connected to rolling mills [8]. In steel industries, many different phases can be identified and a lot of energy is required [9]. Focusing on steel industry reheating furnaces, many plants exploit air and gas for triggering the needed combustion reactions. In order to enhance energy efficiency and to reduce CO<sub>2</sub> emissions in these plants, different software and/or hardware upgrades can be introduced at the different levels of the automation hierarchy [10,11]. In this context, Industry 4.0 and energy efficiency

certificates represent drivers for the development of tailored projects. In order to guarantee the feasibility of a project and a remarkable return on investment (ROI), high energy efficiency performances are required while maintaining the required quality of final products [12,13].

In the last decades, many researchers, engineers, and practitioners tackled the challenge of improving energy efficiency in steel industry reheating furnaces, proposing data analysis, monitoring, and modelization techniques, as well as Advanced Process Control (APC) and optimization software solutions. In some cases, hardware modification strategies were also considered.

In literature, various software innovation solutions can be found. The proposed solutions are based on simulations, controllers, and optimizers; simulation-based solutions are proposed in [14,15], while level 2 control and optimization solutions are reported in [16–24]. Level 1 controllers are proposed in [25–30], while high-level solutions are reported in [31–35].

In [14], simulation methods and artificial intelligence are used for the modelization of electricity and natural gas consumption in a walking furnace. The length of the rolling campaign and the established rolling program are considered in the design of Best Available Techniques. A ternary model for a walking beam continuous reheating furnace is formulated in [15], and a validation is performed exploiting experimental data from trailing thermocouple experiments. A simulator for control purposes is then implemented based on the obtained model.

With regard to level 2 controllers and optimizers, in [16], a billet reheating furnace model is formulated through a genetic algorithm and a nonlinear optimization problem is proposed for the minimization of fuel cost while satisfying a desired discharge temperature. Genetics algorithms are combined with a set of fuzzy rules in [17] for a bloom reheating furnace optimization algorithm taking into account temperature specifications and specific fuel consumption. The proposed system is simulated under different scenarios. In [18], particle swarm optimization algorithms are used for the solution of a multi-objective optimization problem which considers energy consumption, oxidation, and burning loss minimization. In [19], the slabs discharge temperature, the slabs temperature uniformity, and the specific fuel consumption are included in a function value-based multi-objective optimization problem. Hooke–Jeeves direct search algorithm was used to minimize the objective functions under a series of production rates. In [20], mathematical modelization is exploited to design a model-based control and optimization framework for steel slab reheating furnaces, also reporting simulation and field experiments. A nonlinear model predictive controller is designed in [21] for the temperature control of slabs in a reheating furnace. The proposed system is tested through a real industrial application. In [22], a general structure of an optimal control system for heating billets in a reheating furnace before rolling is given while considering energy saving specifications. A dynamic optimizer for temperature control of steel slabs in a continuous reheating furnace is proposed in [23]. The capabilities of the proposed method are demonstrated through a case study. In [24], an optimal heating pattern for the slabs reheating in a furnace is guaranteed taking into account energy consumption.

With regard to level 1 controllers, a distributed Model Predictive Control (MPC) strategy is proposed in [25], exploiting a model which considers the coupling effect between furnace zones. A Generalized Predictive Control (GPC) is used in [26] to optimize fuel consumption in a reheating furnace, and simulations are proposed taking into account different operating conditions. A cross-limiting control strategy for combustion control is proposed in [27] where environmental pollution and energy consumption as Key Performance Indicators (KPIs) are taken into account. In [28], the combustion process is controlled through hybrid intelligent fuzzy and expert techniques taking into account the distinction between fluctuating and stable operating conditions. Industrial experiments are reported. An adaptive neural fuzzy inference is designed in [29] for the cascade control of temperature and flow with a double cross strategy, and tailored simulations are proposed. In [30], a Smith predictor scheme is combined to a fuzzy scheme in order to control the soaking zone temperature in a steel slab reheating furnace.

With regard to high-level solutions, in [31], reference trajectories of furnace zone temperatures are planned, solving a quadratic program that takes into account pieces temperature specifications. Efficiency–temperature relationships of a reheating furnace are identified and exploited in [32] for optimization purposes to search for the most energy-efficient reheating operations by preserving logistics performances. In [33], a review of scheduling and planning methods for steel hot rolling mills is reported, focusing on data availability and optimization methods. A multi-objective optimization formulation is proposed in [34] to obtain and integrate scheduling between a reheating furnace and a hot rolling line. The developed methods are tested through simulated data. Another approach to synchronize a slab reheating furnace and a hot rolling mill is proposed in [35], taking into account the reduction of the dispensable energy consumption and the increase in the production rate of the overall system.

Different hardware innovations are proposed in literature [36–43]. In [36], the challenge to increase the energy efficiency in a natural gas-fired reheating furnace is tackled. For example, plant and measurements improvements are proposed, i.e., furnace pressure tapping modifications and thermocouple relocation. In addition, inter-billet gap readjustment and improvements on the delay and shutdown logics related to the zone temperatures setpoints are designed. In [37], a numerical study verified the enhanced efficiency of a steel reheating furnace when applying oxy–fuel combustion instead of air–fuel combustion. Only radiation heat transfer was considered to analyze the periodically transient slab heating for an axial-fired furnace and to compare the slab heating behavior between air–fuel and oxy–fuel combustion. In [38], a comparison between oxy–fuel, lean oxy–fuel, and air–fuel practices in reheating furnaces is proposed in order to evaluate oxide-scale layer growth and morphology during simulated typical stainless steel slab reheating prior to hot rolling. In [39], an assessment of burners in reheating furnaces is given, focusing on the utilization of by-product combustion gases. In [40], various aspects of oxy–fuel combustion such as heat transfer modes, energy efficiency, and flame–furnace interaction are discussed considering different burners. In [41], the effect of the burner position in a walking beam type reheating furnace is investigated. It is proven how burner position has a great effect on efficiency and heating characteristics, and the obtained results show that the most appropriate burner configuration depends on the geometry of the furnace. In [42], hardware modifications of a pusher type reheating furnace are examined. The research aims to reduce various heat losses through skin losses, excess scale formation, exhaust gas, and air inhalation for achieving high thermal efficiency. In [43], a series of experiments was conducted on a testing facility and a real-scale furnace, for analyzing the nitric oxide emission reduction. The effects of the temperature, oxygen concentration, and amount of secondary combustion air were investigated in a single-burner combustion system. It was proven that the combined application of burner and furnace air-staged combustions facilitated nitric oxide emission reduction.

A synergic combination of hardware and software innovations for energy efficiency and process control improvement in steel industry is proposed in the present work; to the best of the authors' knowledge, this approach is not present in the literature, particularly for steel billets reheating furnaces in rolling mills. The results achieved in terms of APC performance and energy savings confirmed the validity of the proposed approach. The proposed level 2 APC system is based on MPC strategy. The adoption of MPC techniques was made possible since a reliable model of the process was obtained in the modeling phase. The proposed APC system guarantees reliable, real-time control of the considered process. This fact motivated the use of MPC instead of other techniques, e.g., simulation methods or Artificial Intelligence. To the best of authors' knowledge, projects which include implementation on the real process that are designed as lasting control applications and not as temporary tests are not widespread. The field application of a system designed and tested through virtual environment simulations requires significant reliability and robustness features in order to bridge the gap between simulations and field application.

The paper is organized as follows: Section 2 reports the material and methods, providing: steel billets reheating furnaces description (process main features, control, and optimization specifications), and the proposed software and hardware innovations. Section 3 reports the results and discussion, focusing on control and energy efficiency aspects. The conclusions are summarized in Section 4, with some ideas for future work.

## 2. Materials and Methods

### 2.1. Case Study: Process Description and Specifications

The configuration of the studied reheating furnace and rolling mill is depicted in Figure 1. Billets characterized by different geometries (height in the range 130–150 mm, width in the range 170–150 mm, length in the range 11.5–14 m, mass in the range 2100–2350 kg) and different mean inlet temperatures (30–300 °C) are reheated in the reheating furnace. The reheating furnace is pusher type, i.e., the billets' movement takes place through kick-in pushers' action which introduces the next billet into the furnace (no empty spaces are present between the billets) [44–46]. Billets are moved through the furnace from right to left in Figure 1, and at the furnace exit, a kick-out device performs billets' discharge (with a billets' temperature of about 1150–1250 °C). The discharged billets are transported to the rolling mill stands where plastic deformation takes place. Within their path along the furnace, billets are moved through different furnace areas (see Figure 1). Each area may be composed of one or two zones [44–46]. Table 1 reports some detailed features of the furnace, i.e., the furnace areas, the furnace zones within each area, the length of each area, and the billets' number within each area. The preheating area is not equipped with burners, while the other areas are fuel-fired. Areas 1–2 are characterized by a single burners' group, while two groups of burners are present in areas 3–4: in this way, left–right billets' sides can be subjected to different temperatures. This process feature is important because at furnace discharge, the head and the tail of each billet are subjected to a different residence time before rolling.

**Table 1.** Furnace features.

Area	Zones	Length (mm)	Billets' Number
Preheating Area	Preheating Zone	7400	30
Area 1	Zone 1	1600	11
Area 2	Zone 2	3200	23
Area 3	Zone 3 Right, Zone 3 Left	1700	16
Area 4	Zone 4 Right, Zone 4 Left	2100	13

Two groups of rolling mill stands can be observed in Figure 1. The distance between the furnace exit and the first rolling mill stand is about 16 m. This path, in the initial configuration of the plant, was uncovered, so the billets were in direct contact with the outside environment (see Section 2.2.1). The configuration without tunnel is referred as *original* plant configuration.

At the furnace inlet, combustion smoke is sent to a chimney where smoke exchanger temperature is measured through a thermocouple. In addition, an O<sub>2</sub> analyzer is present. Billets' inlet temperature and billets' outlet temperature at rolling mill stands are measured through optical pyrometers. No information is available for billets' temperature and position within the furnace. An ammeter measures the current absorption within the rolling mill stands. Furnace zones temperature is measured through suitable thermocouples; in Figure 1, note that areas 3–4 are equipped with one thermocouple for each zone (left–right). O<sub>2</sub> content is measured in areas 1, 2, and 4. Ambient temperature in the rolling mill stands area is measured through a thermocouple. All the described signals, together with photocells and trigger signals related to the furnace inlet and outlet and to the rolling mill stands, are provided by plant's PLCs (Programmable Logic Controllers) [47].

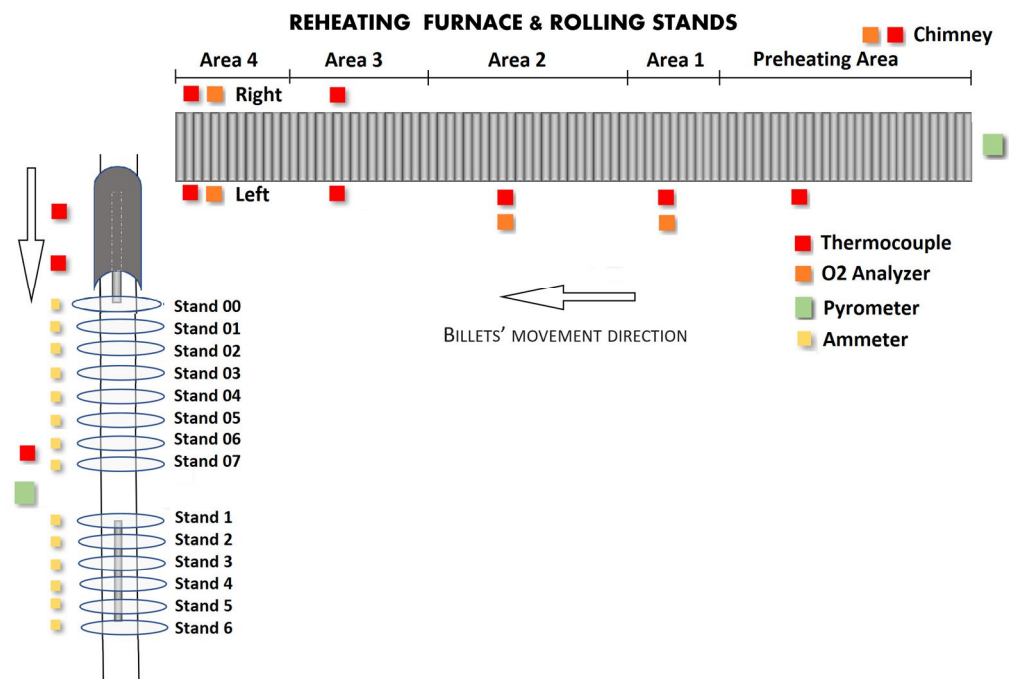


**Figure 1.** Process configuration.

In order to ensure satisfactory control and optimization performances, different specifications have to be considered [46,48]. First, constraints on  $O_2$  content, smoke exchanger temperature, furnace zones temperature, and stoichiometric ratios have to be respected. Second, a correct billet reheating profile must be ensured. Third, temperature difference constraints between left and right zones in areas 3–4 must be met. In this context, fuel flow rate minimization ensures energy efficiency improvement. In the previous furnace conduction, plant operators set the zone temperatures setpoint on the local PID controllers, based on their skills and experience. These controllers were in charge of the computation of the gas content to be injected into the furnace. No temperature and accurate position information was available for plant operators with regard to the billets' behavior during their path within the furnace and in the first part of the rolling mill stands.

In order to implement an APC system, a temperature specification at the rolling mill pyrometer (see Figure 1) was defined. Tables 2–4 report the main Controlled Variables (CVs), Manipulated Variables (MVs,  $u \in R^{l_u \times 1}$ ), and Disturbance Variables (DVs,  $d \in R^{l_d \times 1}$ ) of the proposed APC system (see Section 2.2). It is important to note that the furnace production rate is not manipulated by the APC system in this case study (see Tables 3 and 4). CVs were divided into two groups (see Table 2): billets' temperature at rolling mill stand 07 ( $b \in R^{m_b \times 1}$ ) and furnace variables ( $y \in R^{m_y \times 1}$ ). In the considered case study,  $l_u = 12$ ,  $l_d = 7$ ,  $m_y = 15$ , and  $m_b = 93$ . All the process variables are measured.

**Table 2.** APC CVs.

Variable	Measurement Unit
Rolling Mill Stand 07 Billet Temperature	[°C]
Zone Temperature (4L, 4R, 3L, 3R, 2, 1)	[°C]
Zone Temperatures Difference (4R–4L, 3R–3L)	[°C]
Preheating Zone, Smoke Exchanger Temperature	[°C]
Smoke Exchanger $O_2$	[%]
$O_2$ in Zone 4L, 4R, 2, 1	[%]

**Table 3.** APC MVs.

Variable	Measurement Unit
Zone (4L, 4R, 3L, 3R, 2, 1) Fuel Flow Rate	[Nm <sup>3</sup> /h]
Zone (4L, 4R, 3L, 3R, 2, 1) Air/Fuel Ratio	[–]

**Table 4.** APC DVs.

Variable	Measurement Unit
Furnace Production Rate	[ton/h]
Billets' Furnace Inlet Temperature	[°C]
Warm Air Temperature Valve	[%]
Smoke Exchanger Valve	[%]
Rolling Mill Stands Ambient Temperature	[°C]
Tunnel Temperature 1,2	[°C]

In order to allow the APC system to manipulate the fuel flow rates and the air/fuel ratios of the different furnace zones, modifications on the process automation were needed for the bypass of the output provided by the local PID temperature controllers. In fact, as previously mentioned, before the installation of the proposed APC system, the local PID temperature controllers computed the gas content to be injected into the furnace.

## 2.2. Hardware and Software Innovations

In this section, the hardware and software innovations which were performed on the reheating furnace and on the rolling mill are reported. Hardware innovations refer to the modification of the plant configuration, while software ones refer to the design and the installation of a proprietary APC system based on MPC strategy.

### 2.2.1. Installation of an Insulated Tunnel

A benefit study on the plant was performed to forecast the possible benefits related to the design and the installation of an APC system based on the CVs, MVs, and DVs reported in Tables 2–4. With respect to the *original* plant configuration (see Section 2.1), a hardware modification was proposed in order to guarantee a higher heat retention of the billets before their path along the rolling mill stands. An insulated tunnel was installed on the plant at the furnace exit (see Figure 1). The top of the tunnel includes four covers that can be opened as needed, while the bottom part is characterized by six flaps. The ideal configuration is to keep both covers and flaps closed so as not to waste heat. The covers can be kept closed, but the flaps need to be opened sometimes in order to discharge the scale due to the billets transit. For this reason, an in-depth study was conducted to define intelligent management of flaps' opening mechanism. Two thermocouples were installed inside the tunnel (see Figure 1). Several tests were performed to obtain optimal sensors' placement with respect to measurements reliability. Billets quickly pass through the first part of the tunnel and then their speed is reduced since the billet starts to be rolled into the first stand; while the billet head starts the rolling process, its tail is still in the tunnel (see Figure 1). This difference in speed causes some differences in the measurements: the first thermocouple (closer to the furnace) measures lower temperatures with respect to the second one. In order to include the two thermocouples' information within the APC system design, they are considered as measured DVs (see Table 4). As additional information, it is worth noting that thermocouples in the tunnel may be subjected to breakage caused by the abnormal movement of billets passing too close to them. As will be explained in the following, this fact represented an additional crucial point to be considered in the APC system design.

### 2.2.2. APC Design

An APC system was designed based on the MVs ( $u$ ), DVs ( $d$ ), and CVs ( $b$ ,  $y$ ) reported in Tables 2–4. The APC system is capable of managing all process conditions (normal pro-

duction, planned/unplanned downtimes/shutdowns, restarts) in all plant configurations (with/without tunnel). These features qualified the proposed APC system as a reliable and expert system able to control and optimize all process conditions. The variability and, in some cases, the unpredictability of some events in the considered process (e.g., an unplanned downtime), require efficient handling within the system in order to guarantee the best operating configurations in all process conditions.

Figure 2 reports the APC system scheme. A Supervisory Control And Data Acquisition (SCADA) system acquires plant signals and writes the computed MVs setpoint ( $u(k)$ ). The variables reported in Tables 2–4 are included within the plant signals acquired through the SCADA system. The MVs setpoint is computed by the MPC block (see in the following). As mentioned in Section 2.1, no sensor information is available for billets' temperature and position within the furnace; for this reason, in order to estimate billets' temperature and to track the billets' position, a virtual sensor was designed (see *Virtual Sensor* in Figure 2) [47]. The virtual sensor runs every second within the SCADA system and considers radiation heat transfer within the furnace and convection heat transfer outside the furnace [48,49]. The used radiation model (not reported for brevity, see [48,50]) is nonlinear and its emissivity coefficient is adapted online based on rolling pyrometer measurements at stand 07. The generic discrete-time equation for convection heat transfer related to the  $j$ th billet temperature,  $T_r$ , outside the reheating furnace is ([49]):

$$T_{r,j}(k+1) = T_{r,j}(k) + \beta_{r,j} \cdot (u_{r,j}(k) - T_{r,j}(k)) \text{ [K]} \quad (1a)$$

$$T_{r,j}(0) = T_{f,j}(e_{f,j}) \text{ [K]} \quad (1b)$$

where  $k = 0, \dots, (e_{r,j} - 1)$  is the discrete-time instant,  $e_{r,j}$  is the instant at which the  $j$ th billet will leave the considered rolling mill stands,  $T_{r,j}$  is the mean billet temperature (K), and  $u_{r,j}$  (K) is the (measured) temperature of the rolling mill area where the considered billet transits in the considered discrete-time instant.  $T_{f,j}(e_{f,j})$  is the mean furnace outlet temperature of the billet at the time instant  $e_{f,j}$ .  $e_{f,j}$  is the effective time instant that was associated to the billet's discharge event from the reheating furnace. Note that, in Equations (1a) and (1b), different time instants are associated to the variables  $T_r$  and  $T_f$ .  $u_{r,j}$  represents the ambient temperature that the billet travels through after its discharge from the furnace. The  $\beta_{r,j}$  dimensionless coefficient is represented by:

$$\beta_{r,j} = \frac{T_c \cdot h_j \cdot A_j}{m_j \cdot c_p} \quad (2)$$

where  $T_c$  (s) is the sampling time,  $A_j$  ( $\text{m}^2$ ) is the area of the exposed surface of the  $j$ th billet,  $m_j$  (kg) is the mass of the  $j$ th billet,  $c_p$  ( $\text{J}/(\text{kg} \cdot \text{K})$ ) is the specific heat coefficient of the  $j$ th billet, and  $h_j$  ( $\text{W}/(\text{m}^2 \cdot \text{K})$ ) is the convection coefficient of the  $j$ th billet. All parameters in Equation (2) are assumed to be known except for the convection coefficient. The tuning of this coefficient is performed through a tailored method that exploits operational data and considers different operating conditions. The operational data refer to suitable collection campaigns achieved using portable pyrometers at furnace exit. Equations (1a), (1b) and (2) are derived from the following continuous-time convection equation [49]:

$$\dot{Q}_{conv} = h_j \cdot A_j \cdot (T_{r,j} - u_{r,j}) \text{ [W]} \quad (3)$$

where  $Q_{conv}$  is the thermal power exchanged between the considered billet and the environment in the rolling mill area where the considered billet transits.

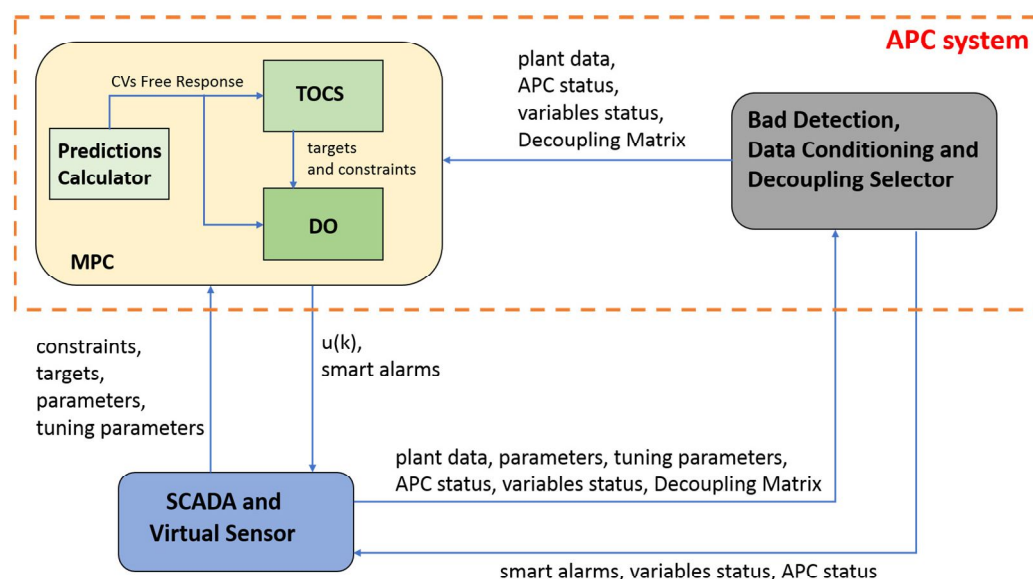


Figure 2. APC system architecture.

$u_{r,j}$  term of Equation (1a) plays a fundamental role in the prediction of the billets' temperature at rolling mill stand 07 (see Figure 1 and Table 2). In order to ensure a reliable  $u_{r,j}$  signal, a bad detection (validity limits, spikes, and freezing checks) and filtering algorithm was designed in order to select and define the reliable thermocouples measurements among the three ambient thermocouples in the rolling mill stands area (see Table 4). These thermocouples are located in the rolling mill stands area: the first was placed far from heat sources, while the other two thermocouples are inside the tunnel (see Figure 1 and Section 2.2.1). After assessing the reliable thermocouples measurements in the rolling mill stands area, the  $u_{r,j}$  real-time signal is computed as the mean of the filtered reliable thermocouples measurements. This capability of the proposed system to robustly and reliably identify the thermocouples measurements for the computation of  $u_{r,j}$  real-time signal represents the key for the synergy between the proposed hardware and software innovations. Thanks to the installation of the insulated tunnel at the end of the reheating furnace, the heat power demand within the furnace is lowered at the same boundary conditions (e.g., furnace production rate). This information is fully exploited within the proposed APC system through the robust and reliable computation of the mean temperature of the rolling mill environment in which the billets transit when they exit the furnace. The obtained synergy between hardware and software innovations has been based on a reliable tunnel installation at the end of the furnace and, at the same time, on a reliable installation of the two thermocouples within the tunnel (see Table 4). In addition, the temperature signals provided by the two thermocouples are exploited within the proposed software innovation which consists on the design of a level 2 APC system based on MPC strategy (see in the following).

The convection model reported in Equations (1a) and (1b) is used to translate temperature specifications at stand 07 to specifications at furnace exit, while the radiation model is used to predict billet temperature at furnace exit. In the furnace areas equipped with two thermocouples (see Figure 1 and Section 2.1), a mean of the acquired temperatures is considered as input of the radiation model.

Billets' temperature at rolling mill stand 07 ( $b$  CVs, see Section 2.1) is predicted through the formulated nonlinear model suitably linearized for MPC purposes, obtaining a Linear Parameter Varying (LPV) model [48,50,51]. The furnace CVs ( $y$  CVs, see Section 2.1) are predicted through First-Order Plus Deadtime (FOPDT) models obtained through a black-box identification approach [52]. Among furnace CVs, zone temperatures are also exploited as intermediate variables between the MVs and the billet temperature model. In this way, a relationship between the MVs and the billets' temperature ( $b$  CVs, see Section 2.1) is obtained, and it is exploited for control and optimization purposes. Billets'

temperature ( $b$  CVs, see Section 2.1) feedback provided by the optical pyrometer at rolling mill stand 07 (see Figure 1) is exploited through the formulated radiation heat transfer model which considers the previously mentioned adaptation policy of the emissivity coefficient. In addition, furnace CVs feedback is exploited by implementing a deadbeat Kalman filter [53,54].

The APC system (see Figure 2) runs with a sampling time equal to 1 min within the SCADA system and is characterized by different blocks, e.g., *Bad Detection*, *Data Conditioning and Decoupling Selector*, and *MPC* (see Figure 2). The first one defines the control matrix and the desired decoupling policies through suitable status values (see Figure 2): based on the current conditions, subsets of MVs, CVs, and DVs can be excluded from the controller formulation [46]. For example, when the virtual sensor estimates the billets' temperature poorly, the billets' temperature at rolling mill stand 07 ( $b$ ) is not considered by the *MPC* block. In this way, two main control modes are obtained: with and without the whole group of  $b$  CVs [50]. The use of MPC was motivated by the reliability of the obtained process model. The *MPC* block exploits a receding horizon strategy, and it is composed of a prediction module (*Predictions Calculator*, see Figure 2) and a two-layer MPC scheme, characterized by a Dynamic Optimizer (*DO*), and a Targets Optimizing and Constraints Softening (*TOCS*) module (see Figure 2). In order to ensure robustness of furnace production rate changes, suitable adaptation laws of the MPC prediction horizon  $H_p$ , control horizon  $H_u$ , and input move blocking instants  $M_i$  ( $i = 1, \dots, H_u$ ) were designed [50,55,56]. As mentioned in Section 2.1, the furnace production rate is a DV in the proposed APC system control matrix. Based on the adapted  $M_i(k)$  instants and on the computed control/prediction horizon, the following parametrization is assumed for MVs predictions at the current control instant  $k$ :

$$\begin{aligned} \hat{u}(k + M_1(k)|k) &= \dots = \hat{u}(k + M_2(k) - 1|k) = u(k - 1) + \Delta\hat{u}(k + M_1(k)|k) \\ \hat{u}(k + M_2(k)|k) &= \dots = \hat{u}(k + M_3(k) - 1|k) = u(k + M_1(k)|k) + \Delta\hat{u}(k + M_2(k)|k) \\ &\vdots \\ \hat{u}(k + M_{H_u}(k)|k) &= \dots = \hat{u}(k + H_p(k) - 1|k) = \hat{u}(k + M_{H_u-1}(k)|k) + \Delta\hat{u}(k + M_{H_u}(k)|k) \end{aligned} \quad (4)$$

where  $u(k - 1)$  is the MVs setpoint at the previous control instant.

*DO* Quadratic Programming (QP) and *TOCS* Linear Programming (LP) formulations are reported in the following (the interested reader can see [48,57,58] for further details). The *DO* QP problem cost function to be minimized is:

$$\begin{aligned} V_{DO}(k) &= \sum_{i=0}^{H_p-1} \|\hat{u}(k + i|k) - u_t(k + i|k)\|_{S(i)}^2 + \sum_{i=1}^{H_p} \|\hat{y}(k + i|k) - y_t(k + i|k)\|_{Q(i)}^2 \\ &\quad + \sum_{i=1}^{H_u} \|\Delta\hat{u}(k + M_i|k)\|_{R(i)}^2 + \|\varepsilon_y(k)\|_{\rho_y}^2 \\ &\quad + \sum_{j=1}^{m_b} \|\hat{b}_j(k + \hat{e}_j(k|k)|k) - b_{t_j}\|_{P_j}^2 + \|\varepsilon_b(k)\|_{\rho_b}^2 \end{aligned} \quad (5)$$

subject to the linear constraints

$$lb_{duDO}(i) \leq \Delta\hat{u}(k + M_i|k) \leq ub_{duDO}(i), \quad i = 1, \dots, H_u \quad (6a)$$

$$lb_{uDO}(i) \leq \hat{u}(k + M_i|k) \leq ub_{uDO}(i), \quad i = 1, \dots, H_u \quad (6b)$$

$$lb_{yDO}(i) - \gamma_{lb_{yDO}}(i) \cdot \varepsilon_y(k) \leq \hat{y}(k + i|k) \leq ub_{yDO}(i) + \gamma_{ub_{yDO}}(i) \cdot \varepsilon_y(k), \quad i = 1, \dots, H_p \quad (6c)$$

$$lb_{b_{DOj}} - \gamma_{lb_{DOj}} \cdot \varepsilon_{bj}(k) \leq \hat{b}_j(k + \hat{e}_j(k|k)|k) \leq ub_{b_{DOj}} + \gamma_{ub_{DOj}} \cdot \varepsilon_{bj}(k), \quad (6d)$$

$$j = 1, \dots, m_b$$

$$\varepsilon_y(k) \geq 0; \varepsilon_b(k) \geq 0. \quad (6e)$$

In Equation (5),  $\|\cdot\|$  is the Euclidean norm. The decision variables are the MVs moves included in  $\Delta\hat{u}(k + M_i|k)$  vectors and the slack variables included in  $\varepsilon_y(k)$  and  $\varepsilon_b(k)$  vectors. All the terms of Equations (5) and (6a)–(6e) are parametrized with respect to the decision variables and to the known terms at each control instant  $k$ , e.g., the MVs setpoint at the previous control instant  $u(k-1)$ . The MPC formulation contains the tracking error terms for MVs and CVs; the tracking errors are weighted in Equation (5) through suitable positive semi-definite matrices ( $S(i)$  and  $Q(i)$ ) and non-negative parameter  $P_j$ . Move suppression term is present in Equation (5); the MVs moves are suitably weighted through positive definite  $\mathcal{R}(i)$  matrices. Among tracking error terms, for each  $j$ th  $b$  CV, a temperature target  $b_{t_j}$  at its furnace discharge predicted instant  $\hat{e}_j$  is defined.

With regard to the constraints reported in Equations (6a) and (6e), different types of constraints have been included. MVs magnitude constraints in Equation (6a) are *hard*, together with the MVs moves constraints in Equation (6b). *Hard* constraints cannot be violated, and their feasibility has been suitably imposed. CVs constraints are *soft* (see Equations (6c) and (6d)), both for the furnace CVs and for the billets temperature CVs; the constraints relaxation can be obtained, when needed, through  $\varepsilon_y(k)$  and  $\varepsilon_b(k)$  non-negative slack variables vectors (see Equation (6e)). In the CVs constraints, the slack variables are multiplied by suitable coefficients  $\gamma$  (see Equations (6c) and (6d)), while, in the cost function (5), they are weighted through positive definite matrices  $\rho$  [57,58].

The computation of the MVs setpoint to be sent to the plant at each control instant takes place within the *DO* module in the *MPC* block, exploiting the MVs setpoint at the previous control instant  $u(k-1)$  and the computed MVs first move on the control horizon ( $\Delta\hat{u}(k|k)$ ). As mentioned in the previous, the updated MVs setpoint is sent to the plant through the SCADA system (for further details about the proposed process automation architecture, see Section 2.2.3).

The *TOCS* LP problem cost function to be minimized is:

$$V_{TOCS}(k) = c_u^T \cdot \Delta\hat{u}_{TOCS}(k) + \rho_{y_{TOCS}}^T \cdot \varepsilon_{y_{TOCS}}(k) \quad (7)$$

subject to the linear constraints

$$lb_{du_{TOCS}} \leq \Delta\hat{u}_{TOCS}(k) \leq ub_{du_{TOCS}} \quad (8a)$$

$$lb_{u_{TOCS}} \leq \hat{u}_{TOCS}(k) \leq ub_{u_{TOCS}} \quad (8b)$$

$$lb_{y_{TOCS}} - \gamma_{lb_{y_{TOCS}}} \cdot \varepsilon_{y_{TOCS}}(k) \leq \hat{y}_{TOCS}(k) \leq ub_{y_{TOCS}} + \gamma_{ub_{y_{TOCS}}} \cdot \varepsilon_{y_{TOCS}}(k) \quad (8c)$$

$$\varepsilon_{y_{TOCS}}(k) \geq 0. \quad (8d)$$

In the linear cost function (7), the preferred optimization directions for MVs can be imposed through the coefficients included in the  $c_u$  vector since it multiplies the MVs steady-state move  $\Delta\hat{u}_{TOCS}(k)$ .  $ub_{du_{TOCS}}$  and  $lb_{du_{TOCS}}$  terms constrain the MVs steady-state move in Equation (8a), while MVs steady-state magnitude  $\hat{u}_{TOCS}(k)$  is constrained by  $ub_{u_{TOCS}}$  and  $lb_{u_{TOCS}}$  terms in Equation (8b). MVs constraints are *hard*. The *TOCS* decision variables are included in  $\Delta\hat{u}_{TOCS}(k)$  and  $\varepsilon_{y_{TOCS}}(k)$  vectors.  $\varepsilon_{y_{TOCS}}(k)$  contains a set of non-negative slack variables (see Equation (8d)) which produce *soft* constraints  $lb_{y_{TOCS}}$  and  $ub_{y_{TOCS}}$  (see Equation (8c)) on the  $y$  CVs steady-state value  $\hat{y}_{TOCS}(k)$ .  $\varepsilon_{y_{TOCS}}(k)$  contains two non-negative slack variables for each  $y$  CV; it has been introduced in Equation (7) through

$\rho_{y_{TOCS}}$  vector and in Equation (8c) through  $\gamma_{lby_{TOCS}}$  and  $\gamma_{uby_{TOCS}}$  vectors.  $\rho_{y_{TOCS}}$ ,  $\gamma_{lby_{TOCS}}$ , and  $\gamma_{uby_{TOCS}}$  vectors contain positive variables.

As can be observed in Equations (7) and (8a)–(8d), TOCS module formulation exploits  $y$  CVs FOPDT models (see Section 2.2.2) and predictions at the end of the prediction horizon  $H_p$ . The solution of the TOCS module LP problem provides the  $y$  CVs and MVs steady-state targets, and the  $y$  CVs constraints (Figure 2, *targets and constraints*) to be used in the DO module formulation. In this sense, TOCS module represents the upper layer of the designed two-layer MPC scheme, while DO module constitutes the lower layer.

Suitable tuning procedures were used for the tuning of the parameters of the developed TOCS and DO modules. As previously mentioned, an adaptation law was formulated for the online tuning of the prediction horizon, the control horizon, and the input move blocking instants. With regard to the *soft* constraints of Equations (6a)–(6e) and (8a)–(8d), the associated parameters  $\gamma$  and  $\rho$  are set in order to establish the desired priority for constraints satisfaction. With regard to the parameters of the cost functions, e.g., the elements of  $c_u$  vector in TOCS module formulation being set as positive, in order to prefer, when possible, minimization directions for the fuel flow rates and the stoichiometric ratios should occur.

### 2.2.3. Computational Framework

The computational framework used for all the project phases excluding the commissioning phase was represented by a laptop computer with the following specifications: Intel(R) Core(TM) i8-3840QM CPU with 3 GHz HDD. A MATLAB environment was used for data analysis, modelization, and virtual environment simulations. The MATLAB Identification Toolbox, MATLAB Control System Toolbox, and MATLAB Optimization Toolbox were exploited for process identification and MPC synthesis. Furthermore, a MATLAB environment was also used for the project maintenance in order to analyze the system performance and KPIs [59].

For the commissioning phase (field implementation), the architecture shown in Figure 3 was exploited, taking into account the schematic representation of Figure 2. The yellow and orange rectangles were already present in the architecture that characterized the plant before the installation of the proposed hardware and software innovations. PLCs (see orange rectangle) manage level 0 and level 1 of the automation hierarchy. Level 2, previously managed by plant operators (see Section 2.1), runs on the plant SCADA system. The proposed hardware and software innovations include the installation of a proprietary APC and MPC software: this solution is adopted in order to limit the project costs and, at the same time, guarantee the needed and desired customization for the considered process. The APC and MPC software run on an additional SCADA system (see blue rectangle in Figure 3) which is installed into an industrial PC server located on the plant. Thanks to the options provided by the adopted SCADA system, plant operators can manage and monitor the proposed software through a client PC installed in the control room (see green rectangle in Figure 3). In the proposed architecture, plant information (e.g., sensors measurements and plant signals) is provided to the APC system by PLCs and plant SCADA. On the other hand, the APC system sends the computed MVs values to the plant PLCs through the SCADA system present on the PC server. The MVs values are computed by the MPC system (see Figure 2). In addition, thanks to the additional options provided by the adopted SCADA system, a set of smart alarms was defined. The specific architecture has been successful in achieving Industry 4.0 compliance for the developed APC system.

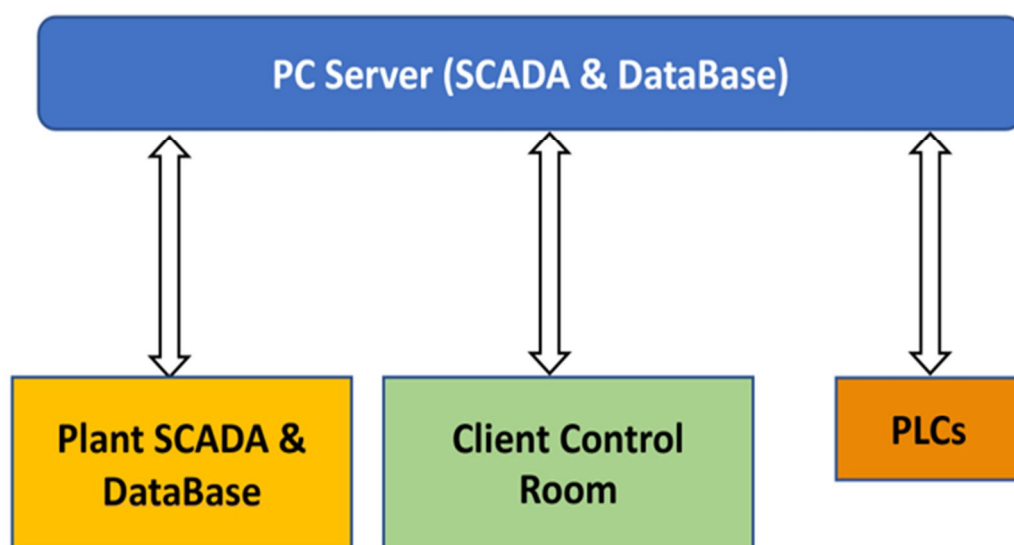


**Figure 3.** Architecture for data exchange in the real plant.

### 3. Results and Discussion

The project was divided into two parts. The first part ended with the commissioning of the APC system without tunnel installation. The tunnel was subsequently installed and the updated APC system was commissioned. The APC system replaced the previous control system based on operators' manual management of the local PID temperature controllers.

#### 3.1. Control Results

Different performance tests were executed on the plant, comparing trends with/without APC system in conditions with/without insulated tunnel. Figures 4–15 report a performance test with/without APC system executed with the insulated tunnel installed. A time period of 19 h is selected: in the first 6 and a half hours, the APC system is off. The APC system flag is reported through a horizontal green line in all the figures; to make it clearer, a vertical black line has also been added to all the figures, to specify the time when the APC system was turned on. Figure 4 reports the billets' temperature measured by the rolling mill stand 07 pyrometer (red), together with the estimation provided by the virtual sensor (blue) and the desired constraints (red dashed/dotted lines). Figures 5–8 report the main DVs. Furnace area temperatures are reported in Figure 9; their constraints are not reported for brevity. Fuel flow rate MVs setpoints are depicted in Figures 10–15 (blue) together with their constraints (red). As can be noted, the desired billets' constraints are not satisfied with the previous furnace conduction (see Figure 4). As previously explained, during the previous plant conduction, no information was available about the temperature of the billets during their path within the furnace and in the first part of their path within the rolling mill stands. In addition, the inconstant DVs (see Figures 5–8) increase the difficulty of the control and optimization problem; in fact, as can be noted in Figures 5 and 7, the furnace production rate and the billets' furnace inlet temperature are not constant. As a result, in the previous furnace conduction, a large standard deviation is noticed in Figure 4 (left side) with regard to the billets' rolling mill stand 07 temperature; in addition, the defined constraints (see red lines in Figure 4) are often violated, thus compromising the quality of the final product. With the activation of the proposed APC system, despite DVs changing conditions (see Figures 5–8), the standard deviation of the billets' rolling mill stand 07 temperature is reduced and a satisfactory behavior is obtained (see Figure 4). Acceptable small violations of the defined constraints are obtained and, when possible, the defined temperature lower constraint at stand 07 (see dotted line in Figure 4) is approached. This behavior of the process inferred by the proposed APC system contributes to a specific fuel consumption reduction (see Section 3.2). The APC system, manipulating the fuel flow

rates (see Figures 10–15) and using furnace area temperatures (see Figure 9) as intermediate variables, successfully regulates the furnace. As can be noted in Figures 10–15, the APC system fully exploits the allowed range of the fuel flow rates (see the defined constraints represented through red lines in Figures 10–15): this is an important difference with respect to the previous furnace conduction in which only a limited range is used for fuel flow rates values. This fact also causes an extension of the exploited range in the trends of the furnace area temperatures (see Figure 9).

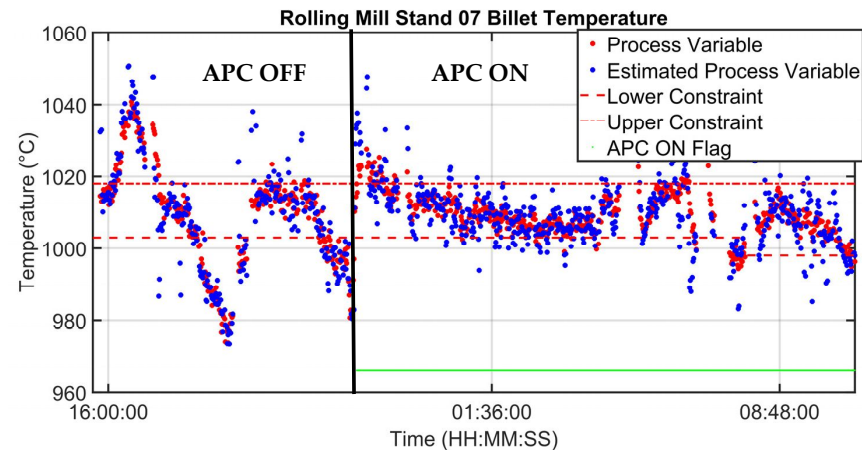


Figure 4. Field results: CVs—rolling mill stand 07 billet temperature.

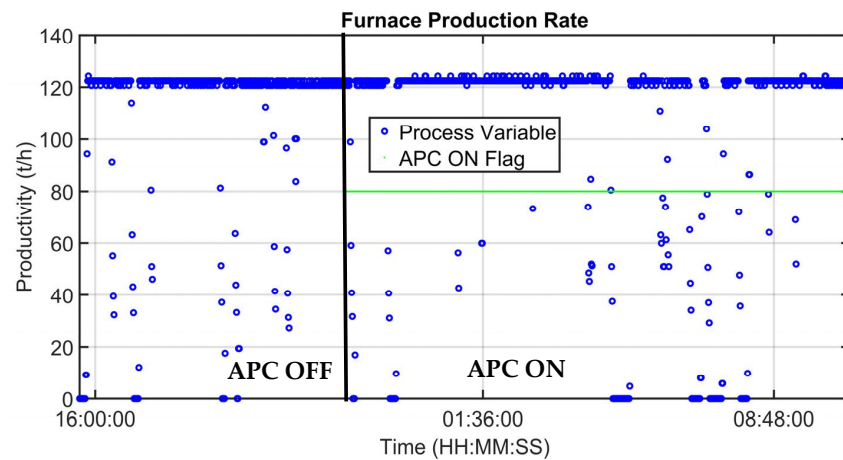


Figure 5. Field results: DVs—furnace production rate.

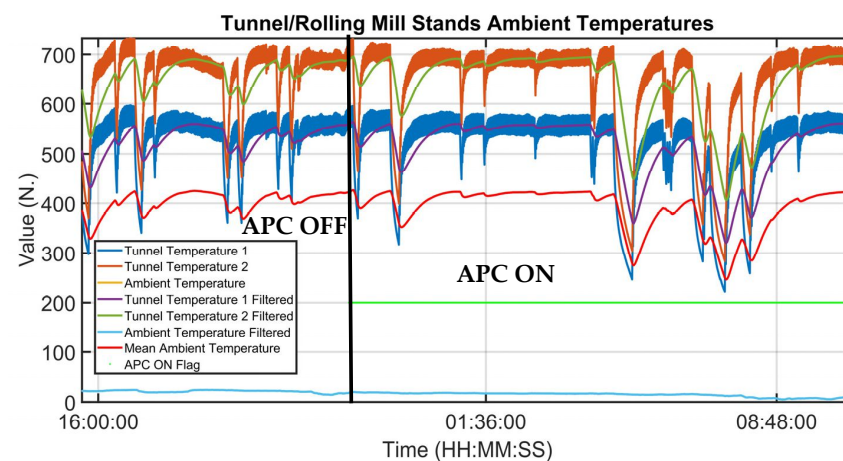


Figure 6. Field results: DVs—tunnel/rolling mill stands ambient temperature.

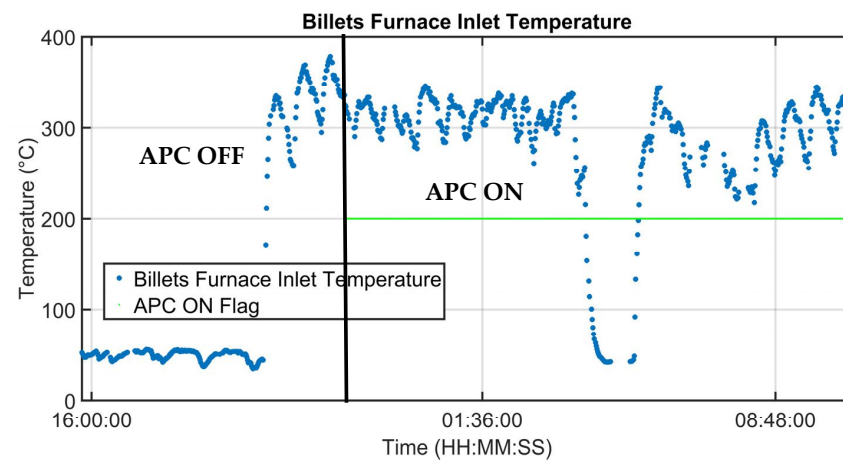


Figure 7. Field results: DVs—billets' furnace inlet temperature.

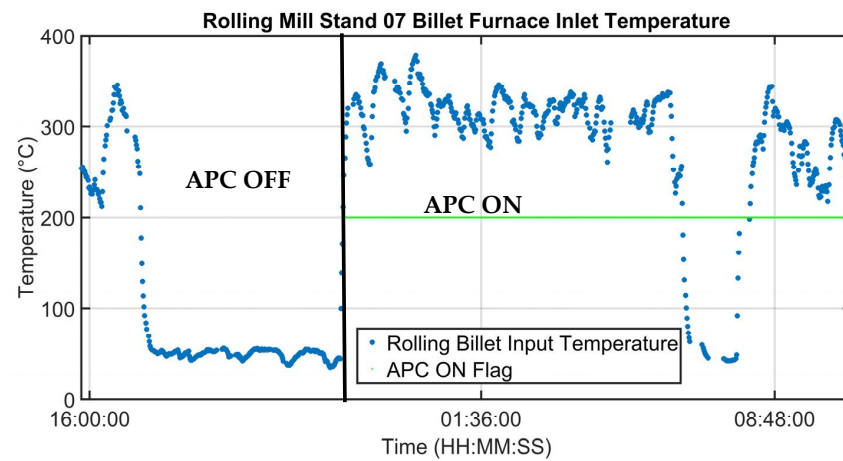


Figure 8. Field results: DVs—rolling mill billet furnace inlet temperature.

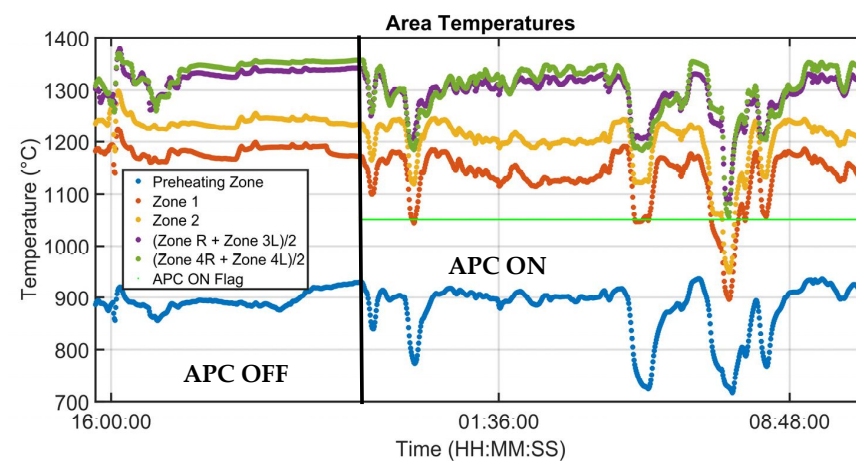


Figure 9. Field results: CVs—area temperatures.

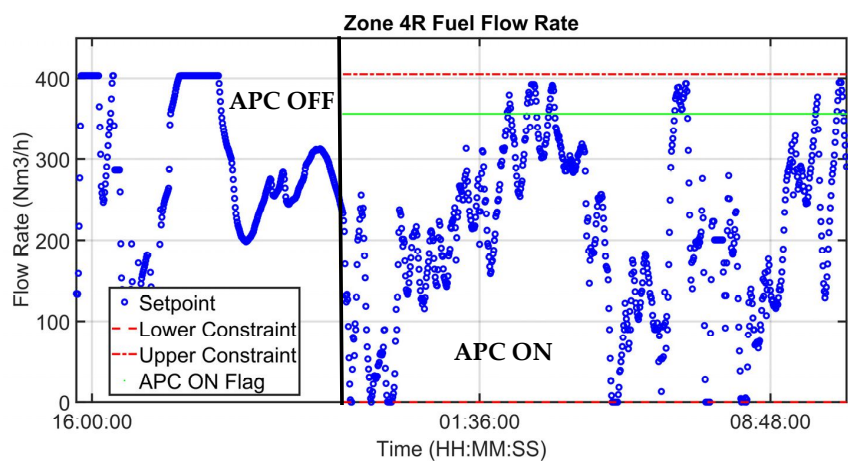


Figure 10. Field results: MVs—fuel flow rate 4R.

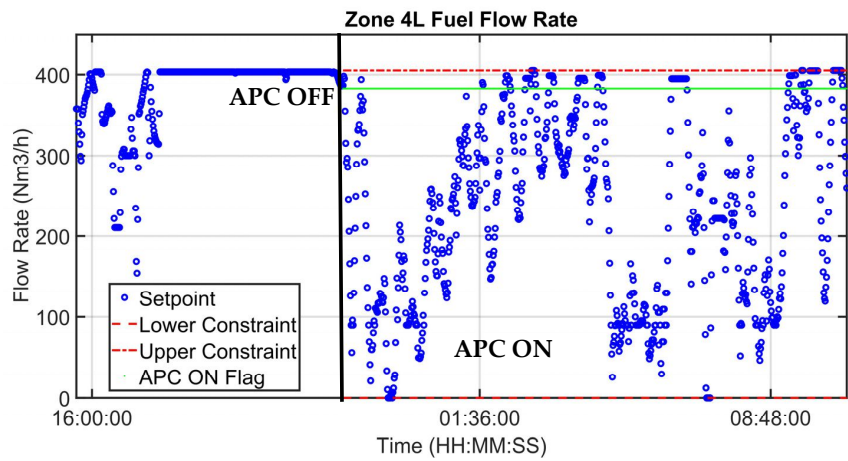


Figure 11. Field results: MVs—fuel flow rate 4L.

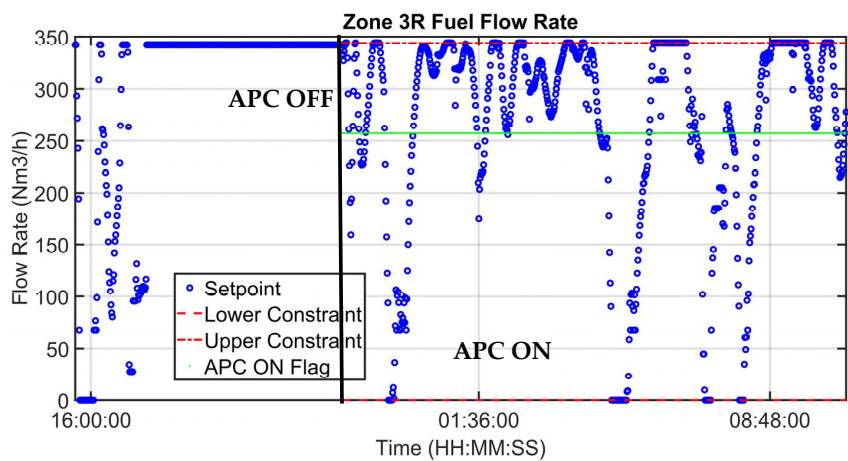


Figure 12. Field results: MVs—fuel flow rate 3R.

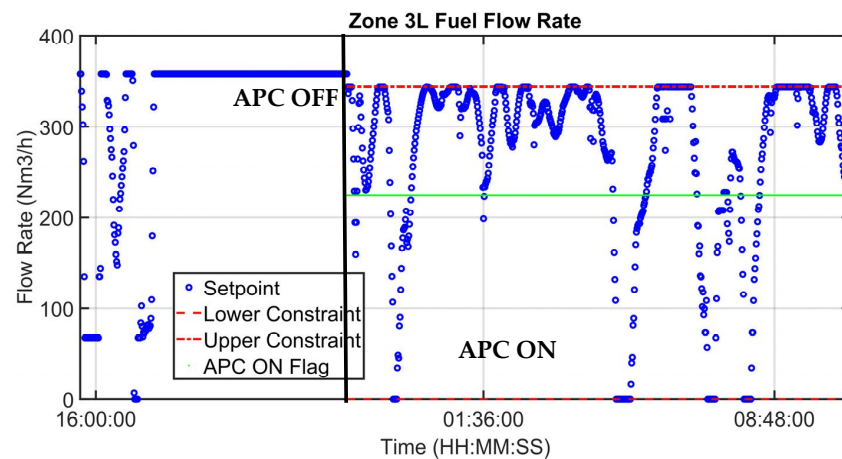


Figure 13. Field results: MVs—fuel flow rate 3L.

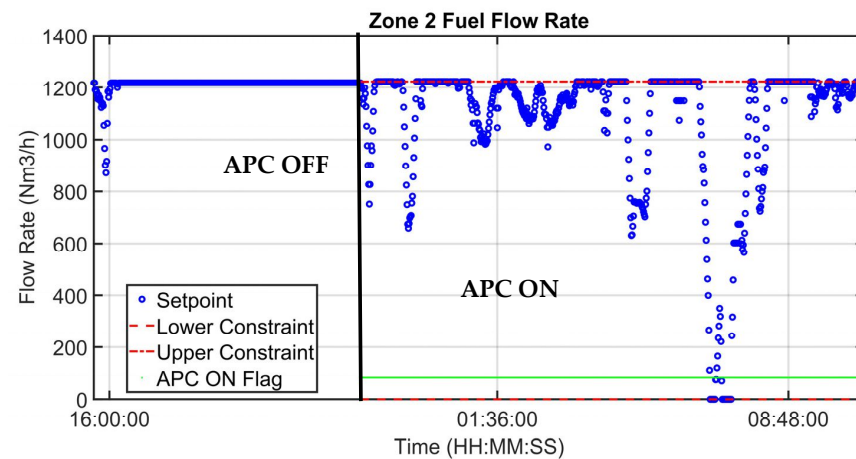


Figure 14. Field results: MVs—fuel flow rate 2.

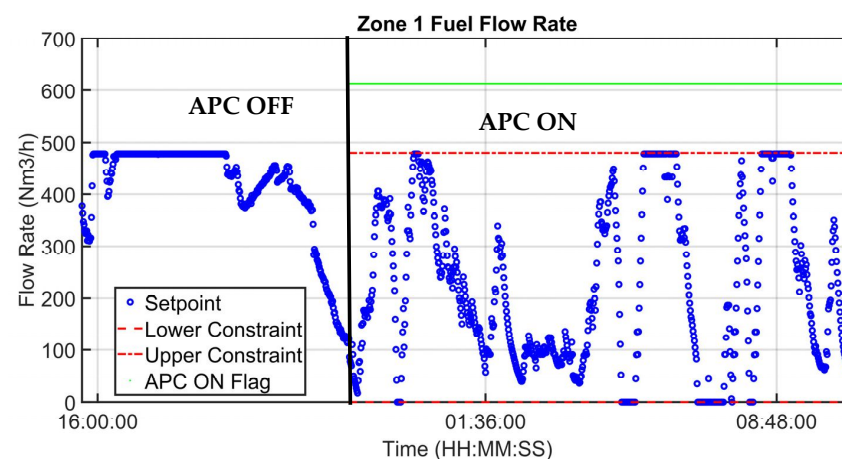


Figure 15. Field results: MVs—fuel flow rate 1.

With regard to the insulated tunnel and rolling mill stands thermocouples, Figure 6 shows the used mean ambient temperature (red line): this temperature is computed as the mean of the reliable ambient temperatures; because in the selected period, all ambient temperature sensors measurements are reliable (i.e., no bad detection flag is verified for them), and the virtual sensor fully exploits this information for the computation of the mean ambient temperature used in Equation (1a). This procedure contributes to a very good fit of billets' temperature estimation at rolling mill stand 07 (see blue line in Figure 4):

reliable data and reliable data processing procedures can infer reliable modelization; reliable modelization can infer reliable process control and optimization.

### 3.2. Energy Efficiency Improvement Results

A project baseline was created for energy efficiency improvement evaluation and certification. Fuel specific consumption was selected as the KPI. This key design choice was motivated by the fact that this KPI takes into account both the fuel consumption and the production magnitude of the process. Before the implementation of the proposed hardware and software innovations on the process, the considered reheating furnace is characterized by a yearly average production equal to about 565k ton and by a yearly average fuel consumption equal to about 15,900k Sm<sup>3</sup>. The yearly average fuel consumption corresponds to about 13,120 toe (toe: tonne of oil equivalent). The considered process is energy-intensive and it falls into the steel industry sector which is an “hard-to-abate” sector. Figure 16 reports an example of monthly (blue) and yearly (red) energy saving improvement of the developed project. Up until now, a service factor greater than 95% was achieved, together with an approximately 3% specific fuel consumption reduction. Taking into account the previously mentioned yearly average fuel consumption of about 13,120 toe, the proposed hardware and software innovations achieved an highly evaluable result. The obtained performance ensures a reduction of CO<sub>2</sub> emissions while guaranteeing the required quality standards of the final product. This result was inferred by the synergic combination of the hardware and software innovations: the hardware innovation, i.e., the installation of the insulated tunnel, provides process optimal conditions which require a lower thermal energy within the furnace. The software innovation, i.e., the design and implementation of a proprietary APC package based on MPC strategy, fully exploits the potential given by the tunnel installation and, at the same time, improves the previous furnace conduction.

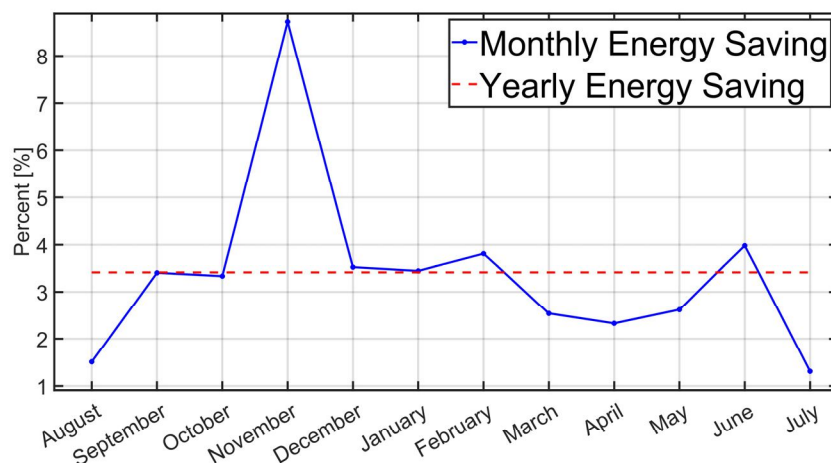


**Figure 16.** Field results: energy efficiency improvement through fuel specific consumption reduction.

## 4. Conclusions

The present paper investigated hardware and software innovations in a steel industry billets’ reheating furnace in order to obtain process control and energy efficiency improvement. The hardware innovation was related to the installation of an insulated tunnel at the end of the reheating furnace, in order to guarantee a higher heat retention of the billets before their path along the rolling mill stands. The software innovation was the design and installation of an Advanced Process Control system based on Model Predictive Control strategy. The Advanced Process Control system replaced the previous control system based on operators’ manual management of the local PID temperature controllers. Up until now, a service factor greater than 95% was achieved, together with an approximately 3% specific fuel consumption reduction. In addition, the developed system received the Industry 4.0 certification.

Future work will be focused on the study, design, and implementation of other modelization and control techniques on the considered plant, exploiting the designed virtual environment simulator to test the developed solutions. In addition, fault detection techniques will be investigated for the steel plants ([60]) and an attempt to extend the developed system to other areas of the steel plants and to other types of reheating furnaces will be performed.

**Author Contributions:** Conceptualization, S.M.Z. and C.P.; Data curation, S.M.Z., C.P. and L.O.; Formal analysis, S.M.Z. and C.P.; Investigation, S.M.Z. and C.P.; Methodology, S.M.Z. and C.P.; Software, S.M.Z. and C.P.; Validation, S.M.Z. and C.P.; Visualization, S.M.Z. and C.P.; Writing—original draft, S.M.Z. and C.P.; Writing—review and editing, S.M.Z. and C.P. All authors have read and agreed to the published version of the manuscript.

**Funding:** This research was supported in part by “EUREKA Project” co-funded by Università Politecnica delle Marche, Regione Marche and i.Process srl.

**Data Availability Statement:** Not applicable.

**Conflicts of Interest:** The authors declare no conflict of interest.

## References

1. Directive 2009/28/EC of the European Parliament and of the Council of 23 April 2009. On the Promotion of the Use of Energy from Renewable Sources and Amending and Subsequently Repealing Directives 2001/77/EC and 2003/30/EC (Text with EEA Relevance). Available online: <http://data.europa.eu/eli/dir/2009/28/oj> (accessed on 4 July 2022).
2. Agenda 2030. Available online: <https://unric.org/it/agenda-2030/> (accessed on 11 August 2022).
3. Sechi, S.; Giarola, S.; Leone, P. Taxonomy for Industrial Cluster Decarbonization: An Analysis for the Italian Hard-to-Abate Industry. *Energies* **2022**, *15*, 8586. [CrossRef]
4. Cavaliere, P. *Clean Ironmaking and Steelmaking Processes: Efficient Technologies for Greenhouse Emissions Abatement*; Springer: Cham, Switzerland, 2019. [CrossRef]
5. Wu, M.; Cao, W.; Chen, X.; She, J. *Intelligent Optimization and Control of Complex Metallurgical Processes*; Springer: Singapore, 2020. [CrossRef]
6. Zanolli, S.M.; Barboni, L.; Cocchioni, F.; Pepe, C. Advanced process control aimed at energy efficiency improvement in process industries. In Proceedings of the 2018 IEEE International Conference on Industrial Technology (ICIT), Lyon, France, 20–22 February 2018. [CrossRef]
7. Zanolli, S.M.; Pepe, C.; Rocchi, M.; Astolfi, G. Application of Advanced Process Control techniques for a cement rotary kiln. In Proceedings of the 2015 19th International Conference on System Theory, Control and Computing (ICSTCC), Cheile Gradistei, Romania, 14–16 October 2015. [CrossRef]
8. Holappa, L. Challenges and Prospects of Steelmaking towards the Year 2050. *Metals* **2021**, *11*, 1978. [CrossRef]
9. He, K.; Wang, L.; Li, X. Review of the Energy Consumption and Production Structure of China’s Steel Industry: Current Situation and Future Development. *Metals* **2020**, *10*, 302. [CrossRef]
10. Schmitz, N.; Sankowski, L.; Kaiser, F.; Schwotzer, C.; Echterhof, T.; Pfeifer, H. Towards CO<sub>2</sub>-neutral process heat generation for continuous reheating furnaces in steel hot rolling mills—A case study. *Energy* **2021**, *224*, 120155. [CrossRef]
11. Zhao, J.; Ma, L.; Zayed, M.E.; Elsheikh, A.H.; Li, W.; Yan, Q.; Wang, J. Industrial reheating furnaces: A review of energy efficiency assessments, waste heat recovery potentials, heating process characteristics and perspectives for steel industry. *Process Saf. Environ. Prot.* **2021**, *147*, 1209–1228. [CrossRef]
12. Astolfi, G.; Barboni, L.; Cocchioni, F.; Dai Prè, M.; Manganotti, D.; Orlietti, L.; Pepe, C.; Zanolli, S.M. Optimization of Steel Industry Billets Reheating Furnaces: An EPC-Based APC Approach. In Proceedings of the 7th International Congress on Science and Technology of Steelmaking: The Challenge of Industry 4.0, Venice, Italy, 13–15 June 2018; Available online: <https://www.scopus.com/record/display.uri?eid=2-s2.0-85062062626&origin=resultslist&sort=plf-f> (accessed on 26 August 2022).
13. Govender, E.; Telukdarie, A.; Sishi, M.N. Approach for Implementing Industry 4.0 Framework in the Steel Industry. In Proceedings of the 2019 IEEE International Conference on Industrial Engineering and Engineering Management (IEEM), Macao, China, 15–18 December 2019. [CrossRef]
14. Niekurzak, M.; Mikulik, J. Modeling of Energy Consumption and Reduction of Pollutant Emissions in a Walking Beam Furnace Using the Expert Method—Case Study. *Energies* **2021**, *14*, 8099. [CrossRef]
15. Yi, Z.; Su, Z.; Li, G.; Yang, Q.; Zhang, W. Development of a double model slab tracking control system for the continuous reheating furnace. *Int. J. Heat Mass Transf.* **2017**, *113*, 861–874. [CrossRef]
16. Santos, H.S.O.; Almeida, P.E.M.; Cardoso, R.T.N. Fuel Costs Minimization on a Steel Billet Reheating Furnace Using Genetic Algorithms. *Model. Simul. Eng.* **2017**, *2017*, 2731902. [CrossRef]
17. Hu, Y.; Tan, C.K.; Broughton, J.; Roach, P.A.; Varga, L. Model-based multi-objective optimisation of reheating furnace operations using genetic algorithm. *Energy Procedia* **2017**, *142*, 2143–2151. [CrossRef]

18. Ding, J.G.; Kong, L.P.; Guo, J.H.; Song, M.X.; Jiao, Z.J. Multi-Objective Optimization of Slab Heating Process in Walking Beam Reheating Furnace Based on Particle Swarm Optimization Algorithm. *Steel Res. Int.* **2020**, *92*, 2000382. [CrossRef]
19. Gao, B.; Wang, C.; Hu, Y.; Tan, C.K.; Roach, P.A.; Varga, L. Function Value-Based Multi-Objective Optimisation of Reheating Furnace Operations Using Hooke-Jeeves Algorithm. *Energies* **2018**, *11*, 2324. [CrossRef]
20. Steinböck, A. *Model-Based Control and Optimization of a Continuous Slab Reheating Furnace*; Shaker Verlag GmbH: Aachen, Germany, 2011.
21. Steinboeck, A.; Wild, D.; Kugi, A. Nonlinear model predictive control of a continuous slab reheating furnace. *Control Eng. Pract.* **2013**, *21*, 495–508. [CrossRef]
22. Andreev, S. System of Energy-Saving Optimal Control of Metal Heating Process in Heat Treatment Furnaces of Rolling Mills. *Machines* **2019**, *7*, 60. [CrossRef]
23. Steinboeck, A.; Graichen, K.; Kugi, A. Dynamic Optimization of a Slab Reheating Furnace With Consistent Approximation of Control Variables. *IEEE Trans. Control Syst. Technol.* **2011**, *19*, 1444–1456. [CrossRef]
24. Jang, J.Y.; Huang, J.B. Optimization of a slab heating pattern for minimum energy consumption in a walking-beam type reheating furnace. *Appl. Therm. Eng.* **2015**, *85*, 313–321. [CrossRef]
25. Nguyen, X.M.; Rodriguez-Ayerbe, P.; Lawayeb, F.; Dumur, D.; Mouchette, A. Temperature control of reheating furnace based on distributed model predictive control. In Proceedings of the 2014 18th International Conference on System Theory, Control and Computing (ICSTCC), Sinaia, Romania, 17–19 October 2014. [CrossRef]
26. Carhuavilca, L.A.; Castro, E.N.; Rodriguez, A.L.; Esparta, D.B. A Comparison of GPC and Fuzzy Smith Predictor for Temperature Control of Steel Slab Reheating Furnace. In Proceedings of the 2021 IEEE XXVIII International Conference on Electronics, Electrical Engineering and Computing (INTERCON), Lima, Peru, 5–7 August 2021. [CrossRef]
27. Zenghuan, L.; Guangxiang, H.; Lizhen, W. Optimization of Furnace Combustion Control System Based on Double Cross-Limiting Strategy. In Proceedings of the 2010 International Conference on Intelligent Computation Technology and Automation, Changsha, China, 11–12 May 2010. [CrossRef]
28. Feng, Y.; Wu, M.; Chen, L.; Chen, X.; Cao, W.; Du, S.; Pedrycz, W. Hybrid Intelligent Control Based on Condition Identification for Combustion Process in Heating Furnace of Compact Strip Production. *IEEE Trans. Ind. Electron.* **2022**, *69*, 2790–2800. [CrossRef]
29. Xiaohua, L.; Yashuai, W.; Yunhai, L. Research on the intelligent temperature control based on ANFIS for reheating furnace in rolling steel line. In Proceedings of the 27th Chinese Control and Decision Conference (2015 CCDC), Qingdao, China, 23–25 May 2015. [CrossRef]
30. Benitez, I.O.; Rivas, R.; Feliu, V.; Sanchez, L.P.; Sanchez, L.A. Fuzzy Gain Scheduled Smith Predictor for Temperature Control in an Industrial Steel Slab Reheating Furnace. *IEEE Lat. Am. Trans.* **2016**, *14*, 4439–4447. [CrossRef]
31. Steinboeck, A.; Graichen, K.; Wild, D.; Kiefer, T.; Kugi, A. Model-based trajectory planning, optimization, and open-loop control of a continuous slab reheating furnace. *J. Process Control* **2011**, *21*, 279–292. [CrossRef]
32. Zaroni, S.; Ferretti, I.; Zavanella, L.E. Energy savings in reheating furnaces through process modelling. *Procedia Manuf.* **2020**, *42*, 205–210. [CrossRef]
33. Özgür, A.; Uygün, Y.; Hütt, M.T. A review of planning and scheduling methods for hot rolling mills in steel production. *Comput. Ind. Eng.* **2021**, *151*, 106606. [CrossRef]
34. Li, K.; Tian, H. Integrated Scheduling of Reheating Furnace and Hot Rolling Based on Improved Multiobjective Differential Evolution. *Complexity* **2018**, *2018*, 1919438. [CrossRef]
35. Ilmer, Q.; Haeussler, S.; Missbauer, H. Optimal Synchronization of the Hot Rolling Stage in Steel Production. *IFAC-Pap.* **2019**, *52*, 1615–1619. [CrossRef]
36. Chakravarty, K.; Kumar, S. Increase in energy efficiency of a steel billet reheating furnace by heat balance study and process improvement. *Energy Rep.* **2020**, *6*, 343–349. [CrossRef]
37. Han, S.H.; Lee, Y.S.; Cho, J.R.; Lee, K.H. Efficiency analysis of air-fuel and oxy-fuel combustion in a reheating furnace. *Int. J. Heat Mass Transf.* **2018**, *121*, 1364–1370. [CrossRef]
38. Laukka, A.; Heikkinen, E.-P.; Fabritius, T. The Atmosphere's Effect on Stainless Steel Slabs' Oxide Formation in a CH<sub>4</sub>-Fuelled Reheating Furnace. *Metals* **2021**, *11*, 621. [CrossRef]
39. Caillat, S. Burners in the steel industry: Utilization of by-product combustion gases in reheating furnaces and annealing lines. *Energy Procedia* **2017**, *120*, 20–27. [CrossRef]
40. Gangoli, S.; Buragino, G.; He, X.; Arslan, E.; Verderame, P.; Hendershot, R.; Slavejkov, A.; Bellis, F.; Bellis, L.; McCarthy, J.; et al. Importance of Control Strategy for Oxy-Fuel Burners in a Steel Reheat Furnace. In Proceedings of the AISTech 2013, Pittsburgh, PA, USA, 6 May 2013; Available online: <https://www.airproducts.de/-/media/airproducts/files/en/335/335-13-010-us-importance-of-control-strategy-for-oxy-fuel-burners.pdf> (accessed on 30 November 2022).
41. Garcia, A.M.; Colorado, A.F.; Obando, J.E.; Arrieta, C.E.; Amell, A.A. Effect of the burner position on an austenitizing process in a walking-beam type reheating furnace. *Appl. Therm. Eng.* **2019**, *153*, 633–645. [CrossRef]
42. Hariramani, S.K.; Yadav, V.; Bansal, R. Energy Conservation Measures in Pusher-Type Reheating Furnace through Modifications and Modernization. In Proceedings of the 2nd International Seminar On “Utilization of Non-Conventional Energy Sources for Sustainable Development of Rural Areas” (ISNCESR '16), Bhilai, Chhattisgarh, India, 17–18 March 2016; Available online: <https://www.ijsr.net/conf/PARAS16/Mech-06.pdf> (accessed on 30 November 2022).
43. Sung, Y.; Kim, S.; Jang, B.; Oh, C.; Jee, T.; Park, S.; Park, K.; Chang, S. Nitric Oxide Emission Reduction in Reheating Furnaces through Burner and Furnace Air-Staged Combustions. *Energies* **2021**, *14*, 1599. [CrossRef]

44. Trinks, W.; Mawhinney, M.H.; Shannon, R.A.; Reed, R.J.; Garvey, J.R. *Industrial Furnaces*; Wiley Online Library: New York, NY, USA, 2003. [[CrossRef](#)]
45. Mullinger, P.; Jenkins, B. *Industrial and Process Furnaces. Principles, Design and Operation*; Elsevier: Amsterdam, The Netherlands, 2014. [[CrossRef](#)]
46. Zanolli, S.M.; Pepe, C.; Barboni, L. Application of Advanced Process Control techniques to a pusher type reheating furnace. *J. Phys. Conf. Ser.* **2015**, *659*, 012014. [[CrossRef](#)]
47. Zanolli, S.M.; Pepe, C.; Moscoloni, E.; Astolfi, G. Data Analysis and Modelling of Billets Features in Steel Industry. *Sensors* **2022**, *22*, 7333. [[CrossRef](#)]
48. Zanolli, S.M.; Cocchioni, F.; Pepe, C. MPC-based energy efficiency improvement in a pusher type billets reheating furnace. *Adv. Sci. Technol. Eng. Syst. J.* **2018**, *3*, 74–84. [[CrossRef](#)]
49. Cengel, Y.A. *Introduction to Thermodynamics and Heat Transfer*; McGraw-Hill Higher Education: New York, NY, USA, 2009.
50. Zanolli, S.M.; Cocchioni, F.; Pepe, C. Model Predictive Control with horizons online adaptation: A steel industry case study. In Proceedings of the 2018 European Control Conference (ECC), Limassol, Cyprus, 12–15 June 2018. [[CrossRef](#)]
51. Mohammadpour, J.; Scherer, C.W. *Control of Linear Parameter Varying Systems with Applications*; Springer: New York, NY, USA, 2012. [[CrossRef](#)]
52. Ljung, L. *System Identification. Theory for the User*; Prentice-Hall PTR: Upper Saddle River, NJ, USA, 1999.
53. Muske, K.R.; Badgwell, T.A. Disturbance modeling for offset-free linear model predictive control. *J. Process Control* **2002**, *12*, 617–632. [[CrossRef](#)]
54. Pannocchia, G.; Rawlings, J.B. Disturbance models for offset-free model predictive control. *AIChE J.* **2003**, *49*, 426–437. [[CrossRef](#)]
55. Cagienard, R.; Grieder, P.; Kerrigan, E.C.; Morari, M. Move blocking strategies in receding horizon control. *J. Process Control* **2007**, *17*, 563–570. [[CrossRef](#)]
56. Maciejowski, J.M. *Predictive Control with Constraints*; Prentice-Hall, Pearson Education Limited: Harlow, UK, 2002.
57. Zanolli, S.M.; Pepe, C.; Rocchi, M. Control and optimization of a cement rotary kiln: A model predictive control approach. In Proceedings of the 2016 Indian Control Conference (ICC), Hyderabad, India, 4–6 January 2016. [[CrossRef](#)]
58. Zanolli, S.M.; Pepe, C.; Rocchi, M. Cement Rotary Kiln: Constraints Handling and Optimization via Model Predictive Control Techniques. In Proceedings of the 2015 5th Australian Control Conference (AUCC), Gold Coast, QLD, Australia, 5–6 November 2015; Available online: <https://ieeexplore.ieee.org/document/7361950> (accessed on 26 August 2022).
59. MathWorks. Available online: <https://it.mathworks.com/> (accessed on 30 November 2022).
60. Zanolli, S.M.; Astolfi, G. Application of a Fault Detection and Isolation System on a Rotary Machine. *Int. J. Rotating Mach.* **2013**, *2013*, 189359. [[CrossRef](#)]

**Disclaimer/Publisher’s Note:** The statements, opinions and data contained in all publications are solely those of the individual author(s) and contributor(s) and not of MDPI and/or the editor(s). MDPI and/or the editor(s) disclaim responsibility for any injury to people or property resulting from any ideas, methods, instructions or products referred to in the content.